Available online at www.sciencedirect.com
ScienceDirect
International Journal of Heat and Mass Transfer 51 (2008) 4811–4819
International Journal of HEAT and MASS TRANSFER
www.elsevier.com/locate/ijhmt

Parametric study of multi-splat solidification/remelting including contact resistance effects

Wei Wang, Ruth A. Lambert, Roger H. Rangel *

Department of Mechanical and Aerospace Engineering, University of California, Irvine, CA 92697-3975, USA

Received 27 July 2007; received in revised form 24 February 2008
Available online 16 April 2008

Abstract

Solidification and remelting behavior of a series of deposited splats is investigated through numerical modeling. The non-perfect thermal contact at the interface between the splat and the substrate surface is accounted for by introducing a heat transfer coefficient. The effect of the interfacial thermal contact resistance as well as the effect of splat solidification parameters such as splat superheats, splat thickness, substrate temperature and splat deposition frequency on the resulting remelting depth of the previously solidified layer are discussed. Numerical results show that in the absence of thermal contact resistance between the splat and substrate interface, the remelting depth is underestimated. It is also found that the remelting depth increases for either an increase in substrate temperature or increasing splat thickness. In addition, the findings in the present study imply that in some practical applications, decreasing the deposit frequency would be a valid method to ensure the constant remelting thickness for depositing layers.
© 2008 Elsevier Ltd. All rights reserved.

Keywords: Solidification of droplets; Contact resistance; Droplet deposition; Rapid solidification; Remelting depth

1. Introduction

Rapid prototyping (RP) is a process in which an arbitrary three-dimensional physical object is built directly from CAD data without the need for molds or tools [1]. Droplet-based solid freeform fabrication (SFF) proposed at UCI is a molten droplet-based additive to RP technology. A conceptual schematic of the droplet-based SFF technique is shown in Fig. 1. Molten droplets on the order of 100 μm in diameter are generated via capillary stream breakup. The charge tube induces a unique charge to each droplet and the deflection plates then deflect the droplets proportionally at rates up to 20,000 droplets per second. Lateral motion of the *x–y* table from CAD information coupled with droplet deflection allows sequential deposition of the molten droplets to fabricate a useful structure layer by layer. Droplet-based SFF is currently capable of producing near net-shape metal components. It is also anticipated that droplet-based SFF will yield fully net-shape components for a variety of useful applications. As droplet-based SFF requires less machine steps than conventional manufacturing techniques, it has the potential to provide improved manufacturing quality and significant economic benefit [2].

The usefulness of the droplet-based SFF technique is determined by the structural characteristics of the material component synthesized. Understanding of the phase-change characteristics of the sequentially deposited droplets during the SFF process is crucial to control and improve the microstructure and hence the structural integrity of the part [3]. A droplet deposition scheme that insures the previously deposited droplets completely solidify before the next droplet arrives is essential for the acquisition of geometric integrity. In order to achieve sufficient bonding between previously solidified layers and those newly arrived, conditions which cause the newly arriving droplet to locally remelt a thin layer of previously deposited and solidified layer are sought. Remelting promotes

* Corresponding author. Tel.: +1 949 824 4033; fax: +1 949 824 8585.
E-mail address: rhrangel@uci.edu (R.H. Rangel).

0017-9310/$ - see front matter © 2008 Elsevier Ltd. All rights reserved.
doi:10.1016/j.ijheatmasstransfer.2008.02.015

Nomenclature

a	splat radius, characteristic length (m)
c_p	specific heat (J/kgK)
f	deposit frequency (s^{-1})
h	heat transfer coefficient (J/sm^{2}K)
h^*	dimensionless heat transfer coefficient, ha/k_s
h_c	convection heat transfer coefficient (J/sm^2 K)
k	thermal conductivity (J/smK)
k_{ch}	characteristic thermal conductivity, k_s (J/sm K)
L	latent heat (J/kg)
L^*	dimensionless latent heat, $L/c_{ps}(T_m - T_B)$
q	heat flux (J/sm^2)
q_{ch}	characteristic heat flux, $k_s(T_m - T_B)/a$
s	solid/liquid interface location (m)
t	time (s)
t_{ch}	characteristic time, a^2/α_s (s)
T	temperature (K)
T^*	dimensionless temperature, $(T - T_m)/(T_m - T_B)$
T_B	substrate initial temperature (K)
T_d	droplet initial temperature (K)
y	spatial coordinate normal to the substrate (m)

Greek symbols

α	thermal diffusivity (m^2/s)
ε	emissivity
ρ	density (kg/m^3)
σ	Stefan–Boltzmann constant (W/m^2 K^4)
α_{ch}	characteristic constant, α_s

Subscripts

c	convection
ch	characteristic value
b	substrate
l	liquid
m	melting
r	radiation
s	solid
eff	effective value

Superscript

*	dimensionless variables

inter-layer adhesion by allowing mixing and therefore should minimize elimination [4]. The amount of remelting is a key parameter. With insufficient remelting, the quality of the material can suffer from a poor adhesion between the layers. In the case of too much remelting, the shape of the material can be inaccurate since a thin liquid layer is formed and remains on the top of the substrate [5]. Understanding the solidification and remelting behavior through a series of deposited droplets is the primary motivation of this investigation. Significant effort has previously been directed toward modeling solidification of thermal spays and droplet splats [6–10]. In most of the investigations, only pure melting or solidification is possible, but not sequential remelting and solidification. In general, the sequential remelting and solidification problem presents challenges since the position of the moving solidifying front is an additional unknown variable.

Some aspects of the physics involved in the substrate melting problem have been examined both experimentally, analytically and numerically. Wang et al. [11] proposed operational maps for the melting of a substrate suddenly brought into contact with a thin layer of solidified metal experiencing no motion, focusing therefore on the solidification aspect of the problem. Amon et al. [4] built a one-

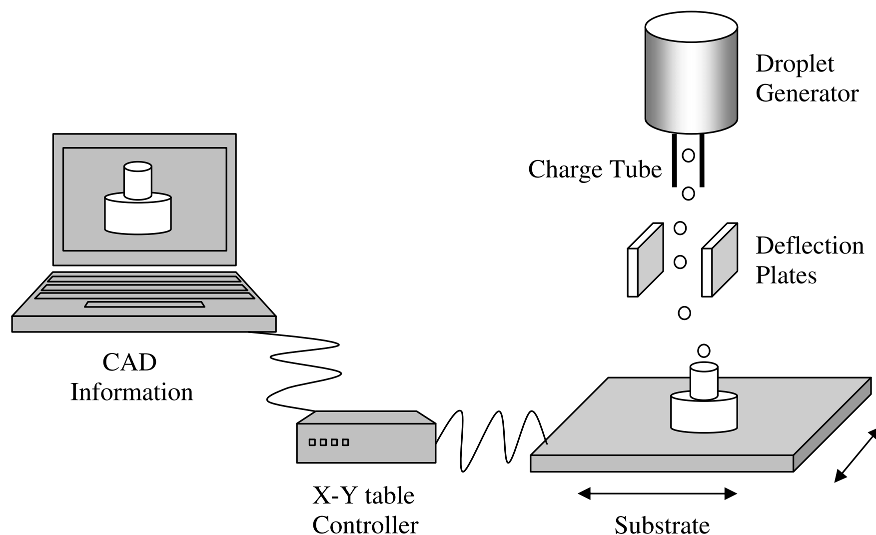

Fig. 1. Schematic of droplet-based SFF apparatus.

dimensional heat conduction model to predict the likelihood of substrate remelting and the maximum remelting depth in micro casting process. Zarzalejo et al. [12] and Schmaltz et al. [13] extended the numerical model of Amon et al. to account for the convective effect of droplet motion through effective thermal conductivity of the liquid metal while the droplet is spreading on the substrate. In addition, the final substrate maximum melting profile was measured by a metallurgical cross-section technique. Rangel and Bian [14] presented a droplet deformation and solidification model which includes a solution of the mechanical energy equation based on the model of Madejski. In addition to addressing the effect of liquid motion on the splat deformation and solidification process, the model can be applied to study the mechanism of substrate remelting. Based on the axisymmetric Lagrangian finite-element formulation of the Navier–Stokes, energy and material transport equations, Attinger and Poulikakos [5] performed numerical investigation of molten microdroplet impact and solidification on a substrate of the same material that melts due to energy input from the impacting material. Hong and Qiu [15] investigated the remelting and resolidification of a substrate caused by molten droplets through numerical modeling considering complex fluid dynamics and thermal contact resistance.

Only a few studies consider the actual remelting behavior through a series of deposited droplets. Kang et al. [16] investigated the remelting phenomena during impact of a droplet on top of a previously solidified one. It was shown that the amount of superheat as well as the variation of thermophysical properties, particularly the latent heat and the melting temperature, influence the degree of remelting of the first solidified droplet. Orme and Huang [3] developed a one-dimensional model to study remelting and solidification characteristics of sequentially deposited droplets utilizing a coordinate transformation to convert the moving boundary into a fixed boundary. The model considered the droplet motion a precursor of thermal processes and thus uncoupled the heat transfer from fluid dynamics phenomenon. In addition, the author omitted thermal contact resistance with the consideration that the substrate makes a perfect contact with the droplet.

Due to the nature of the proposed application, numerical modeling of the remelting behavior through a series of deposited splats is of interest in the present study. We seek to understand the effect of the splat and substrate interface thermal contact resistance on the resulting melting front migration rate, thickness of remelting, and temperature distribution inside both the splat and the substrate. An emphasis will be placed on the effect of splat solidification parameters such as splat superheat, splat thickness, substrate temperature, and splat deposition frequency on the solidification and remelting process. In the numerical model, we will also incorporate convective heat transfer effects through effective thermal conductivity of liquid metal. The effect of the conductivity multiplier on the remelting thickness will be studied. With this knowledge, operating parameters yielding desirable material properties can be optimized.

2. Mathematical formulation and numerical treatment

For the present application of droplet-based SFF, droplets are deposited at high superheats to cause remelting and it is assumed that they spread to flat discs, which is a realistic assumption [3]. Since the physical dimension of the splat in the direction normal to the substrate (height) is small compared to the lateral dimension (width) and the remelting depth is small compared to the splat height, a one-dimensional phase-change simulation is suitable [3]. An order of magnitude analysis shows that the time scale of the spreading process of a drop impacting on a surface is shorter than the time scale of heat transfer process from the splat to the substrate. This relationship implies that the droplets forming the splat spread first and subsequently cool [16]. In order to simplify the numerical simulation and to emphasize the heat transfer aspect of the problem, fluid flow is neglected by taking the droplet spreading as the precursor of the heat transfer. This approach, however, fails to capture the forced convective heat transfer from the droplet to the substrate. In this study, we will multiply the liquid conductivity by a factor greater than one to account for this convective effect [17,12,13]. The liquid conductivity multiplier is defined as, $K_{\text{factor}} = k_{\text{eff}}/k_{\text{l}}$.

The molten splats of thickness a are deposited onto a substrate of thickness of B as illustrated in Fig. 2. Subsequent layers of droplets, M, are deposited on the previously deposited layer. Because the rapid solidification time of the splat is of the order of a microsecond, in most practical circumstances the molten splats will impinge on a layer of previously delivered splat which has already solidified. The model allows the remelting of previous layers, but not of the substrate. The non-perfect thermal contact at the interface between the splat and the substrate surface is quantified by the heat transfer coefficient. When the substrate remelting occurs, however, interface thermal contact resistance between the layers is not incorporated into the model due to the assumption verified by the micrographic examinations that remelting creates a continuous contact

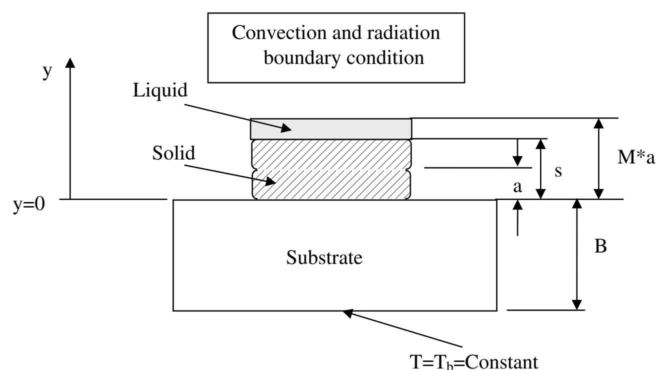

Fig. 2. Schematic diagram of the problem interest.

between the layers [4]. The solid and liquid interface condition assumes the sharp solid to liquid transition of a pure material occurs at the melting temperature [4]. The boundary conditions are convection to the ambient and radiation from a heat source at the top of the splat as illustrated in Fig. 2. Because the substrate is large compared to the splat, the deposited splat does not raise the temperature of the substrate bottom, and the temperature along the substrate bottom is then specified as fixed at the initial substrate temperate.

The equations and boundary conditions governing this problem are written in dimensionless form as

$$\text{Substrate:}\quad \frac{\partial T_b^*}{\partial t^*}=\alpha_b^*\frac{\partial^2 T_b^*}{\partial y^{*2}}\quad \text{for}\quad -\frac{B}{a}>y^*>0 \tag{1}$$

$$\text{Solid:}\quad \frac{\partial T_s^*}{\partial t^*}=\alpha_s^*\frac{\partial^2 T_s^*}{\partial y^{*2}}\quad \text{for}\quad 0<y^*<s^*(t^*) \tag{2}$$

$$\text{Liquid:}\quad \frac{\partial T_l^*}{\partial t^*}=\alpha_l^*\frac{\partial^2 T_l^*}{\partial y^{*2}}\quad \text{for}\quad s^*(t^*)<y^*<M \tag{3}$$

$$\text{Substrate/lower at}\quad y^*=-\frac{B}{a}\quad T_b^*=-1 \tag{4}$$

Substrate/solid at $y^*=0$

$$\text{Substrate top}\quad -k_b^*\frac{\partial T_b^*}{\partial y^*}=h^*(T_s^*-T_b^*) \tag{5}$$

$$\text{Solid bottom}\quad -k_s^*\frac{\partial T_s^*}{\partial y^*}=h^*(T_s^*-T_b^*) \tag{6}$$

Solid/liquid at $y^*=s^*(t^*)$

$$T_s^*=T_l^*=0\quad\text{and}\quad k_s^*\frac{\partial T_s^*}{\partial y^*}-k_{\text{eff}}^*\frac{\partial T_l^*}{\partial y^*}=L^*\frac{ds^*}{dt^*} \tag{7}$$

Liquid/upper: at $y^*=M$,

$$k_{\text{eff}}^*\frac{\partial T_l^*}{\partial y^*}=q_r^*+q_c^* \tag{8}$$

$$q_r=\sigma\varepsilon(T_r^4-T_l^4),\ q_c=h_c(T_c-T_l)$$

Solid/upper: at $y^*=M$,

$$k_s^*\frac{\partial T_s^*}{\partial y^*}=q_r^*+q_c^* \tag{9}$$

$$q_r=\sigma\varepsilon(T_r^4-T_s^4),\ q_c=h_c(T_c-T_s)$$

where the radiant and convective temperatures T_r and T_c are taken as the initial droplet temperature, T_d.

When a droplet is delivered to the previously solidified layer, the solid/liquid interface will regress due to the phase-change transition from solidification to remelting. The remelted material will subsequently resolidify. The solid/liquid interface is difficult to track with the fixed grid approach since it may not necessarily fall on a grid point. To overcome this difficulty, a coordinate transformation to convert the moving boundary into a fixed domain was utilized. The grid transformation is illustrated in Fig. 3. The following transformations are introduced:

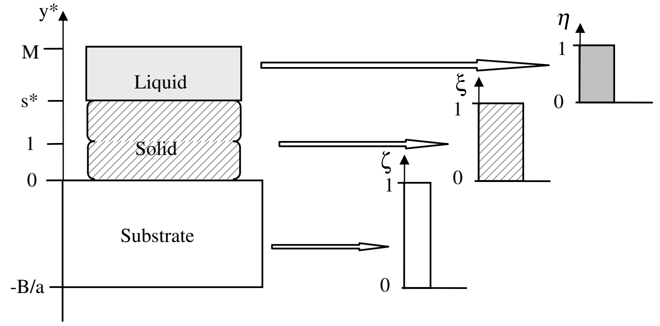

Fig. 3. Transformation from a moving boundary to a fixed boundary.

$$\text{for the solid region:}\quad \xi=\frac{y^*}{s^*}$$

$$\text{for the liquid region:}\quad \eta=\frac{y^*-s^*}{M-s^*}$$

$$\text{for the substrate region:}\quad \zeta=\left(\frac{y^*a}{B}+1\right)^m$$

where m is the spacing parameter. When $m>1$, variable grid spacing with tighter spacing near the substrate/solid boundary is obtained.

Under the above transformation, the governing equations become

Substrate: $0<\zeta<1$

$$\frac{\partial T_b^*}{\partial t^*}=\alpha_b^*\left[\frac{(m^2-m)}{\left(\frac{B}{a}\right)^2}\zeta^{(m-2)/m}\frac{\partial T_b^*}{\partial \zeta}+\left(\frac{ma}{B}\zeta^{(m-1)/m}\right)^2\frac{\partial^2 T_b^*}{\partial \zeta^2}\right] \tag{10}$$

Solid: $0<\xi<1$

$$\frac{\partial T_s^*}{\partial t^*}=\frac{\xi}{s^*}\frac{ds^*}{dt^*}\frac{\partial T_s^*}{\partial \xi}+\frac{\alpha_s^*}{s^{*2}}\frac{\partial^2 T_s^*}{\partial \xi^2} \tag{11}$$

Liquid: $0<\eta<1$

$$\frac{\partial T_l^*}{\partial t^*}=\frac{1-\eta}{M-s^*}\frac{ds^*}{dt^*}\frac{\partial T_l^*}{\partial \eta}+\frac{\alpha_l^*}{(M-s^*)^2}\frac{\partial^2 T_l^*}{\partial \eta^2} \tag{12}$$

The transformed boundary conditions are

$$\text{Substrate/lower:}\quad \zeta=0\quad T_b^*=-1 \tag{13}$$

Substrate/solid: $\zeta=1,\ \xi=0$

$$\text{Substrate top:}\quad -k_b^*\left(\frac{ma}{B}\right)\frac{\partial T_b^*}{\partial \zeta}=h^*(T_s^*-T_b^*) \tag{14}$$

$$\text{Solid bottom:}\quad -k_s^*\left(\frac{ma}{B}\right)\frac{\partial T_s^*}{\partial \zeta}=h^*(T_s^*-T_b^*) \tag{15}$$

Solid/liquid: $\xi=1,\ \eta=0\quad T_s^*=T_l^*=0$

$$\frac{k_s^*}{s^*}\frac{\partial T_s^*}{\partial \xi}-\frac{k_{\text{eff}}^*}{M-s^*}\frac{\partial T_l^*}{\partial \eta}=L^*\frac{ds^*}{dt^*} \tag{16}$$

Liquid/upper: $\eta = 1, s^* < M$

$$\frac{k^*_{\text{eff}}}{M - s^*}\frac{\partial T^*_1}{\partial \eta} = q^*_r + q^*_c \tag{17}$$

Solid/upper: $\xi = 1, s^* = M$

$$\frac{k^*_s}{s^*}\frac{\partial T^*_s}{\partial \xi} = q^*_r + q^*_c \tag{18}$$

The Crank–Nicolson scheme is applied to generate finite difference equations. Since a singularity occurs at $t = 0 (s = 0)$, the Schwarz solution for solidification in an infinite domain [18] is used to initiate the numerical simulation. Detailed studies are dedicated to achieve time and space step-free results. For typical cases a finite difference grid of 300 points is used in the substrate, liquid and solid regions. The time step size that ensures convergence of the numerical solution is chosen for each case.

3. Numerical results and discussion

3.1. Comparison of numerical results with experiment

In order to test the validity of the numerical simulation, numerical results need to be compared with experimental results. However, no experimental data on the solidification and remelting behavior through sequentially deposited layers of splats are available. In this study, experiment results of Zarzalejo et al. [12], which measured the final substrate maximum melting profile by a metallurgical cross-section technique, were transferred here to compare with the numerical simulation results. The case reported by Zarzalejo et al. is the impact of a 3.5 mm stainless steel (SS308) droplet at 2773 K on a flat homogeneous substrate at 300 K. In this case, a maximum substrate remelting depth of 98 μm is measured near the centerline. As shown in Fig. 4, a very clear remelting line below the droplet/substrate interface is apparent. Although the present model allows remelting of previous layers but not of the substrate,

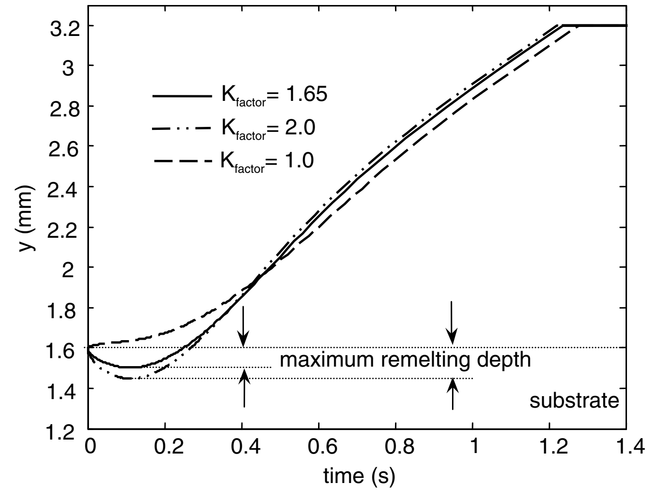

Fig. 5. Moving boundary for two stainless steel (SS308) layers for different K_{factor} values.

the remelting of the substrate could still be predicted if the substrate is made of the same material as that the solidified splat. In the comparison with the experimental results, it is assumed that a layer of previously delivered splat has been solidified and in perfect contact with the substrate which is of the same material. To account for the convective effect in this study, we multiply the liquid conductivity of splat by a factor $K_{\text{factor}} = k_{\text{eff}}/k_1$ greater than one. The position of the moving boundary for two stainless steel (SS308) layers are shown in Fig. 5 for a range in K_{factor} from 1 to 2. The results show that with a conductivity multiplier $K_{\text{factor}} = 1.65$, the maximum remelting depth extends to about 98 μm, which indicates a good agreement with the experimental results of Zarzalejo et al. [12].

3.2. Simulation parameters

As the remelting of the previously solidified splat layer is the primary interest in the present study, we assume the first layer has been deposited and solidified on the substrate

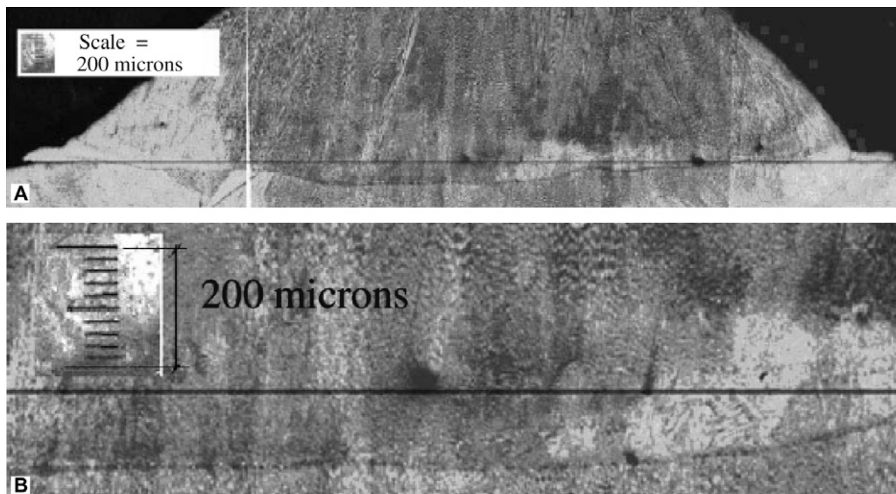

Fig. 4. Experimental results of Zarzalejo et al. [12] illustrating the remelting depth of a stainless steel (SS308) droplet.

Table 1
Material properties for splat and substrate

Material	k (W/m K)	ρ (kg/m^3)	c_p (J/kg K)	L (kJ/kg)	T_m (K)
Copper	397	8960	386		
Solid Al	249	2707	895	402	933
Liquid Al	103	2380	1084	402	933

Table 2
Simulation parameters for the base case

a (μm)	B (mm)	T_B (K)	T_d (K)	f (Hz)	h (W/m^2 K)	K_{factor}
100	25.4	500	1500	150	1×10^5	1.0

at the beginning. Numerical simulations for the solidification and remelting behavior through 2 sequentially deposited layers of splats are conducted. Numerical simulations are presented for typical materials; molten aluminum for the splat liquid and copper for the substrate. The thermal properties of the materials are listed in Table 1 and are assumed to remain constant during the solidification and remelting process. Representative values of droplet size and deposition rates are used and are listed in Table 2 for the base case. In the following discussion, we will present the influence of contact resistance, splat superheat, splat thickness, substrate temperature, deposit frequency and effect of liquid conductivity multiplier on the solidification/remelting process.

3.3. Effect of contact resistance

The effect of contact resistance between the splat and the substrate on the thickness of remelting was studied. The moving boundary history for three layers of aluminum splat under different heat transfer coefficient values: infinite, 2×10^5 W/m^2 K, 1×10^5 W/m^2 K and 8×10^4 W/m^2 K are illustrated in Fig. 6. The evaluation of the temperature at the points located on the top and bottom of the splat and the top of the substrate under different heat transfer coefficients are shown in Fig. 7. For all cases, the superheated molten splat releases an initial sensible heat primarily to the previously deposited layer.

When the splat reaches the liquidus temperature, solidification begins and finishes when the droplet reaches the solidus temperature. This process is followed by splat cooling in the solid phase. As expected, for the lower heat transfer coefficient of $h = 8 \times 10^4$ W/m^2 K, a longer overall solidification time of almost 0.005 s for one entire layer of splat is needed. If the heat transfer coefficient is very high, which means thermal contact resistance is negligible, the previously solidified layer, layer 1 or 2, will not remelt when an additional layer impinges upon it. The absence of remelting due to high values in the heat transfer rate occur since the main thermal resistance is the conduction in the solidified layer. If the thermal conductivity is high, the

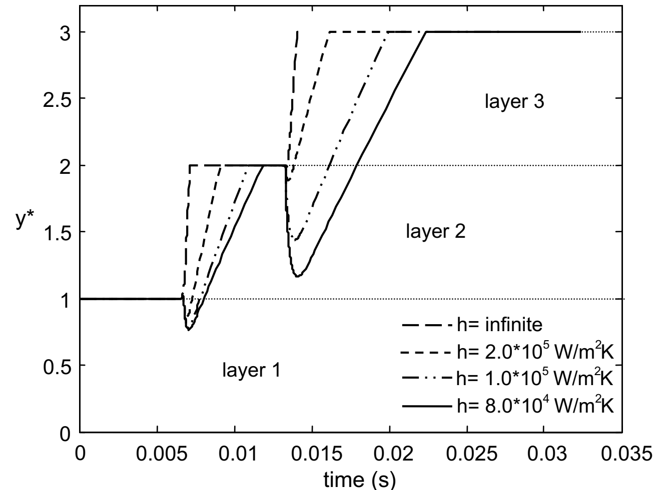

Fig. 6. Moving boundary for three aluminum layers under different heat transfer coefficients.

energy from the newly deposited splat will transport to the substrate very quickly as shown in Fig. 7 thereby raising the temperature of the substrate without remelting the solidified splat layers.

As the value of the heat transfer coefficient decreases, the remelting of the sublayers will increase due in part to the fact that for the lower heat transfer coefficient, the major thermal contact resistance is at the splat/substrate boundary and not in the solidified layer. The thickness of the latter therefore does not influence much the transport of energy from the interface to the substrate because of the high thermal conductivity of aluminum. In this case, the temperature gradient in the solidified layer will be small as shown in Fig. 7b–d. The above results indicate that thermal contact resistance between the splat and the substrate plays a critical role in the remelting of the solidified splat layers and that neglecting this variable can lead to underestimated values of the remelting depth. In all of the following cases, the heat transfer coefficient $h = 1 \times 10^5$ W/m^2 K will be used in the simulation.

3.4. Effect of splat superheat

To characterize the impinging splat superheat effect, we performed numerical simulations varying the initial temperature of the splat within the range of 1200–1800 K. The effect of the splat superheat on the remelting depth is shown in Fig. 8. It can be found that for $T_d = 1200$ K no remelting phenomenon occurs and increasing the superheat will cause the remelting depth to increase. This phenomenon is quite readily understood, because more energy is contained in the impinging splat with a higher superheat.

3.5. Effect of substrate temperature

Numerical simulations were also conducted to study the effect of substrate temperature varying from 200 K to 600 K on the remelting depth. The numerical results are

Fig. 7. Temperature histories at various locations for heat transfer coefficient values, h, equal to (a) infinite, (b) 2×10^5, (c) 1×10^5 and (d) 8×10^4 W/m^2 K.

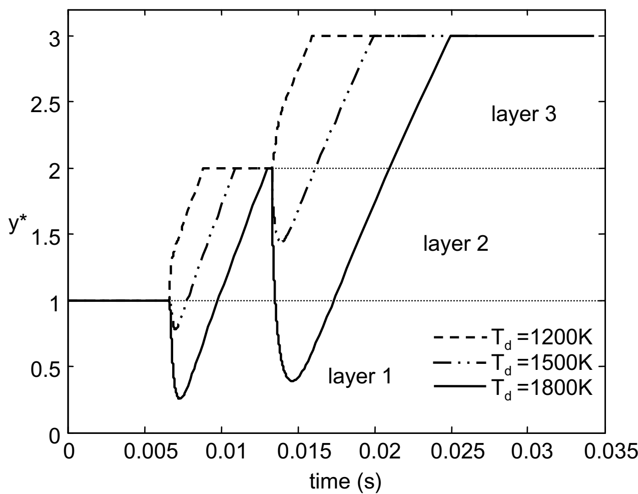

Fig. 8. Moving boundary for three aluminum layers with different superheat values.

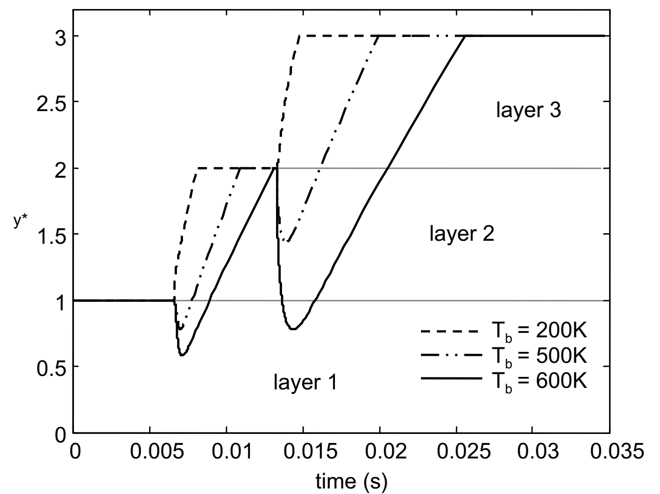

Fig. 9. Moving boundary for three aluminum layers under different substrate temperatures.

presented in Fig. 9. It can be shown that the remelting depth increases with increasing substrate temperature, and that the remelting depth is zero when substrate temperature is the lowest, at 200 K. Remelting increases at higher substrate temperatures since less energy is needed to melt the solidified layer.

3.6. Effect of splat thickness

It is known that the thickness of the splat has a large effect on its average cooling rate and on its final microstructure. The effect of splat thickness on remelting depth, however, has not been fully addressed. Accordingly, we studied the effect of splat thickness on the remelting depth. The splat thicknesses ranged from 50 μm to 120 μm. The numerical simulation results are shown in Fig. 10. The results indicate that the remelting depth of the first layer is almost the same for all cases. This result is reasonable since the largest thermal contact resistance is between the first solidified layer and substrate and not in the solidified layer.

The thickness of solidified layer does not have much influence on the transport of energy from the interface to the substrate due to the high thermal conductivity of aluminum. This, however, is not the case for subsequent layers. The remelting depth of the second layer increases with increasing splat thickness. This increase in remelting depth in the second layer occurs because the interface thermal contact resistance between the layers is not incorporated into the model due to the assumption verified by the micrographic examinations that remelting creates a continuous contact between the layers [4]. More energy is therefore contained in the splat with increased thickness and the transport of energy from additional layers reflects this.

3.7. Effect of deposit frequency

The effect of different deposit frequencies on the moving boundary is shown in Fig. 11. From the simulation results, it can be seen that deposition at short time intervals will increase the remelting depth of the second layer. At short time intervals, the deposit has insufficient time to cool down to the temperature of the previous layer as shown in Fig. 12a resulting in an increase in the remelting depth of layer 2. When the time between layers is sufficient to allow the cooling of layer 2 as indicated in Fig. 12b, the remelting depth of layer 2 will decrease. In practical applications, a constant remelting thickness for sequentially

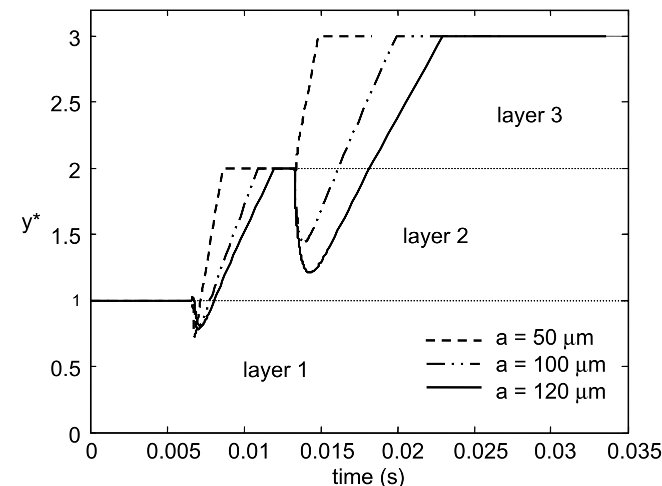

Fig. 10. Moving boundary for three aluminum layers under different splat thickness.

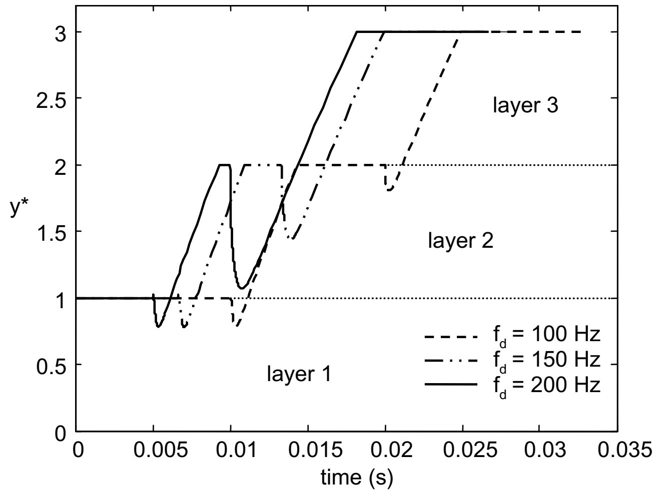

Fig. 11. Moving boundary for three aluminum layers with different deposit frequencies.

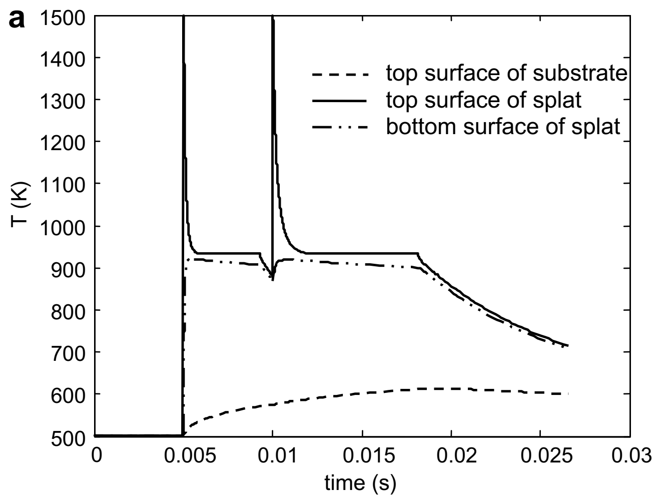

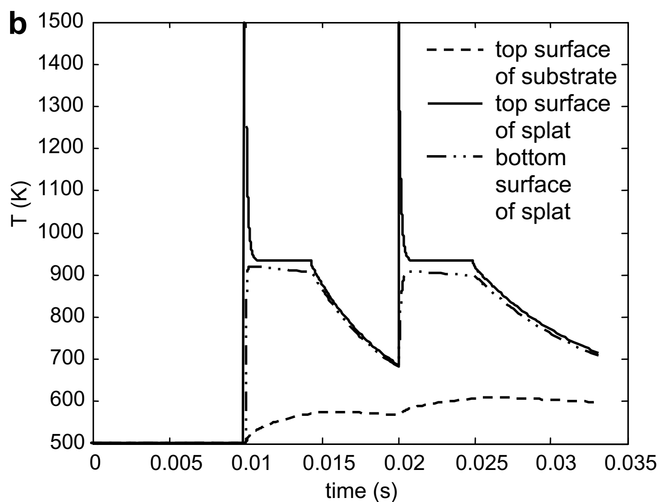

Fig. 12. Temperature histories at various locations for deposit frequencies f_d of (a) 200 and (b) 100 Hz.

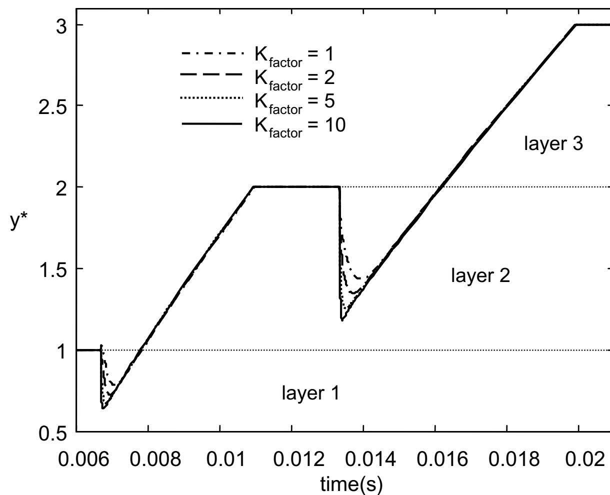

Fig. 13. Moving boundary for three aluminum layers under different values of K_{factor}.

deposited layers is sometimes desired. Because it is difficult to change the droplet temperature or substrate temperature on a layer to layer basis, decreasing the deposit frequency would be a valid method to reduce the variations in remelting depth for different layers.

3.8. Effect of liquid conductivity multiplier

Due to a lack of experimental data to obtain the value of the conductivity multiplier K_{factor}, in the previous sections a value of $K_{factor} = 1.0$ was used in all of the simulations. In order to investigate the effect of K_{factor} on the remelting depth, we performed numerical simulations varying the K_{factor} from 1 to 10. Comparing the results for K_{factor} from 1 to 10 as shown in Fig. 13, we observe that the maximum remelting depth increases as the conductivity multiplier is increased. This result is reasonable since the convective effects promote the occurrence of remelting. The results also show that the absence of convective effects will underestimate the remelting, thus experiments are expected to be conducted in the future to fine-tune the value of the conductivity multiplier.

4. Conclusions

Numerical simulation of solidification and remelting behavior through a series of deposited splats were conducted. The effect of splat/substrate interface thermal contact resistance, and the effect of splat solidification parameters such as splat superheat, substrate temperature, splat thickness, and splat deposition frequency on the resulting remelting depth of the previously solidified layer were investigated. Numerical results show that an increase in contact resistance between the splat and substrate interface results in an increase in remelting depth. This result indicates that neglecting thermal contact resistance will provide results that underestimate the remelting depth. It was also found that both an increase in the splat superheat or substrate temperature and the splat thickness will cause the remelting depth to increase.

For practical applications in which constant remelting depth with subsequent layers is desired, decreasing the deposit frequency achieves this goal. When convective effects are accounted for by multiplying the liquid conductivity by a factor greater than one, it is observed that maximum remelting depth increases as the conductivity multiplier is increased. This indicates that the absence of convective effects will underestimate splat remelting, however further experimentation is needed in order to fine-tune the value of conductivity multiplier. The numerical model designed and presented in this study is a useful tool for optimization of droplet-based FFC process.

References

[1] C. Hull, US Patent No. 6027324, 2000.
[2] M.E. Orme, E.P. Muntz, US Patent No. 5171360, 1992.
[3] M.E. Orme, C. Huang, Phase change manipulation for droplet-based solid freeform fabrication, Trans. ASME J. Heat Transfer 119 (1997) 818–823.
[4] C.H. Amon, K.S. Schmaltz, R. Merz, F.B. Prinz, Numerical and experimental investigation of interface bonding via structure remelting of an impinging molten metal droplet, transactions of the ASME, J. Heat Transfer 118 (1996) 164–172.
[5] D. Attinger, D. Poulikakos, Melting and resolidification of a substrate caused by molten microdroplet impact, transactions of the ASME, J. Heat Transfer 123 (2001) 1110–1122.
[6] H. Liu, E.J. Lavernia, R.H. Rangel, Numerical simulation of substrate impact and freezing of droplets in plasma spay processes, J. Phys. D, Appl. Phys. 26 (1993) 1900–1908.
[7] M. Pasandideh-Fard, S. Chandra, J. Mostaghimi, A three-dimensional model of droplet impact and solidification, Int. J. Heat Mass Transfer 45 (2002) 2229–2242.
[8] S. Kamnis, S. Gu, Numerical modeling of droplet impingement, J. Phys. D, Appl. Phys. 38 (2005) 3664–3673.
[9] C. Le Bot, S. Vincent, E. Arquis, Impact and solidification of indium droplets on a cold substrate, Int. J. Therm. Sci. 44 (2005) 219–233.
[10] W. Wang, F.J. Hong, H.H. Qiu, Prediction of solder bump formation in solder jet packaging processes, IEEE Trans. Components Packag. Technol. 29 (3) (2006) 486–493.
[11] S.-P. Wang, G.-X. Wang, E.F. Matthys, Melting and resolidification of a substrate in contact with a molten metal: operational maps, Int. J. Heat Mass Transfer 41 (10) (1998) 1177–1188.
[12] L.J. Zarzalejo, K.S. Schmaltz, C.H. Amon, Molten droplet solidification and substrate remelting in microcasting – Part I: numerical modeling and experimental verification, Heat Mass Transfer 34 (1999) 477–485.
[13] K.S. Schmaltz, L.J. Zarzalejo, C.H. Amon, Molten droplet solidification and substrate remelting in microcasting – Part II: parametric study and effect of dissimilar materials, Heat Mass Transfer 35 (1999) 17–23.
[14] R.H. Rangel, X. Bian, Metal-droplet deposition model including liquid deformation and substrate remelting, Int. J. Heat Mass Transfer 40 (11) (1997) 2549–2564.
[15] F.J. Hong, H.-H. Qiu, Modeling of substrate remelting, flow, and resolidification in microcasting, Numer. Heat Transfer, Part A 48 (2005) 987–1008.
[16] B. Kang, J. Waldvogel, D. Poulikakos, Remelting phenomena in the process of splat solidification, J. Mater. Sci. 30 (1995) 4912–4925.
[17] M.C. Flemings, Solidification Processing, McGraw-Hill, New York, 1974, pp. 1–328.
[18] H.S. Carslaw, J.S. Jaeger, Conduction of Heat in Solid, second ed., Oxford University Press, Oxford, 1959.